A revised version of this report has been published in *Nature* **489** (2012) 274-277.

Stabilization of Leidenfrost Vapour Layer by Textured Superhydrophobic Surfaces

Ivan U. Vakarelski[1,2], Neelesh A. Patankar[3], Jeremy O. Marston[1], Derek Y. C. Chan[4,5], Sigurdur T. Thoroddsen[1,2]

[1] Division of Physical Sciences and Engineering, King Abdullah University of Science and Technology, Thuwal 23955-6900, Saudi Arabia.
[2] Clean Combustion Research Center, King Abdullah University of Science and Technology, Thuwal 23955-6900, Saudi Arabia.
[3] Department of Mechanical Engineering, Northwestern University, 2145 Sheridan, Evanston IL, USA.
[4] Department of Mathematics and Statistics, University of Melbourne, Parkville 3010, VIC, Australia.
[5] Faculty of Life and Social Sciences, Swinburne University of Technology, Hawthorn 3122, VIC, Australia.

In 1756 Leidenfrost[1] observed that water drops skittered on a sufficiently hot skillet due to levitation by an evaporative vapour film. The stability of such films, only above a critical temperature, is a cornerstone effect in boiling[2]. Low thermal conductivity of the vapour layer inhibit heat transfer in boiling operations, whereas their collapse in cooling applications can result in vapour explosions that are particularly detrimental, for instance in nuclear plants[3]. Vapour films can also reduce liquid-solid drag,[4-6] similar in principle to how a liquid film lubricates the motion of ice skaters. However, the ability to fabricate surfaces that can control vapour film stability remains elusive. Here we show that vapour film collapse does not occur at textured superhydrophobic surfaces. This result fundamentally alters what has been observed for more than two centuries. Whereas at smooth hydrophobic surfaces, the vapour film does collapse, albeit at a lower critical temperature, and switches explosively to nucleate boiling, in contrast, at textured superhydrophobic surfaces, the vapour layer gradually relaxes until the surface is completely cooled, without exhibiting nucleate boiling. This result demonstrates that topological texture on superhydrophobic materials is critical in stabilizing the vapour layer and thus in controlling phase change at surfaces. The concept can potentially be applied to control other phase transitions like ice or frost formation, leading to novel applications to regulate phase behavior using textures[7-9] as well as to the design of novel low drag surfaces at which the vapour phase is stabilized in the grooves of textures without heating[10].

Heat transfer and boiling on a heated solid surface in contact with liquid are familiar phenomena observed in our daily lives and occurs in many industrial processes. As the vessel containing a liquid is heated progressively, the liquid will start to boil with vapour bubbles forming at the hot surface. This is the nucleate boiling regime. If the surface temperature is increased further, a continuous vapour film will form that leads to the film boiling or the Leidenfrost regime. It is known that surface properties such as roughness and wettability can alter the transition temperature from the nucleate to the film boiling regime[11-16]. Since the low thermal conductivity of the vapour layer reduces dramatically the heat transfer efficiency, the traditional focus is to increase the temperature at which the film boiling occurs [13]. However, if the vapour layer is to be used for drag reduction[4-6,17-20], lowering the temperature of film boiling is beneficial because the presence of a Leidenfrost vapour layer can reduce the hydrodynamic drag force on a heated spheres moving in liquid by up to 85%[6].

Takata et al.[12] have reported that the initiation of nucleate boiling can be suppressed at what they termed “super-water-repellent” surfaces. Here we demonstrate that a textured superhydrophobic surface can eliminate the collapse of the vapour film, thus making it possible to maintain a stable vapour film at all temperatures above the boiling point of the liquid, i.e. at all superheats. To this end we investigated cooling and heating phenomena of heated surfaces that possess different degrees of hydrophobicity in water.

In cooling experiments we use 20 mm diameter stainless steel spheres and in heating experiments 24 mm diameter stainless steel cylinders and stainless steel vessels (capacity 60 ml). The surfaces of these are modified to have superhydrophilic, hydrophilic, hydrophobic or superhydrophobic wetting properties as characterized by water drop contact angle in air. The hydrophilic surfaces were produced by cleaning the steel surface with organic solvents that resulted in water contact angles of less than 30º. The hydrophobic surfaces were produced by silanization with trichloro ([1H,1H,2H,2H perfluorooctyl] silane) giving contact angles of about 100º. Superhydrophobic surfaces with water contact angles more than 160º were produced by treatment with a commercial coating agent (Glaco Mirror Coat “Zero”, Soft 99 Co.) containing nanoparticles and organic reagent. Superhydrophilic surfaces, contact angles of less than 10º were produced from the superhydrophobic surface by plasma cleaning to remove the organic coating while retaining the same texture and geometric morphology (See Supplementary Information for details).

An atomic force microscopy image of the superhydrophobic surface coating is shown in Fig. 1a where the rough surface topography is evident. The very high contact angle subtended by a superhydrophobic sphere at the air-water meniscus is shown in Fig. 1b. When fully immersed in water, a silver mirror-like sheen on the sphere surface, due to reflection from the thin air layer retained on the surface, is a signature of the Cassie state[21-24] where water is only in physical contact with the roughness peaks created by the coating (Fig. 1c). This type of air entrapment, called plastron, has been shown to reduce hydrodynamic drag on spheres moving in water[20] and is used by some aquatic insects to facilitate underwater breathing[25].

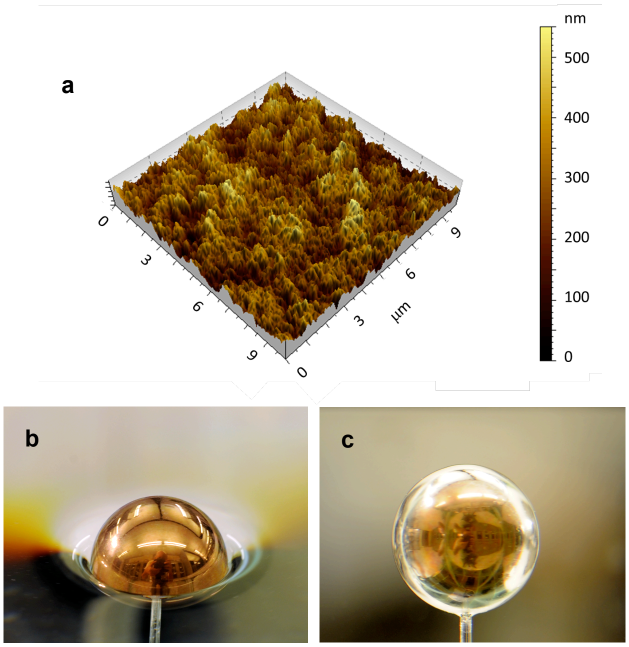

Figure 1 | Surface topography and images of the superhydrophobic sphere. a, 10 μm^2 AFM topography 3D view image of the superhydrophobic surface coating. The combination of high surface roughness with an organic coating provides a high water contact angle > 160°. **b,** Image of the superhydrophobic sphere held on the water surface that illustrates the high contact angle. **c,** Image of the superhydrophobic sphere immersed in water. The silver-mirror sheen of the immersed sphere is due to a thin air layer retained on the sphere surface and is the signature appearance of a Cassie state of the water adjacent to the surface. Further details on the preparation and characterization of the superhydrophobic coating can be found in the Supplementary Information (Supplementary Fig. 1 and Fig. 2.)

We study the cooling of superhydrophilic, hydrophilic, hydrophobic and superhydrophobic spheres that have been pre-heated in a temperature-controlled furnace and then immersed in a glass tank filled with water at 22 °C. The state of the water at the sphere surface during subsequent cooling is captured on high-speed video and the sphere temperature is monitored by an inserted thermo-couple probe thermometer. The progress of the cooling events for the hydrophilic, hydrophobic and superhydrophobic spheres can be seen in Supplementary Movies 1, 2 and 3, respectively. The superhydrophilic and hydrophilic spheres were heated to a maximum temperature of 700 °C but the maximum temperatures that the hydrophobic and superhydrophobic spheres could be raised were limited to about 400 ºC by the thermal stability of the organic coating. For the superhydrophilic sphere the maximum temperature was not high enough to initiate film-boiling and it cooled almost instantaneously accompanied by a vigorous release of bubbles as soon as it came into contact with the water. For all other surfaces, the initial sphere temperatures were high enough to be in the film-boiling regime in which a continuous vapour layer coated the spheres with a single bubble dome formed on the top of the sphere by buoyancy effects. During the initial stage of cooling, this bubble would grow and pinch off periodically from this dome (Fig. 2a). On cooling further, the film-boiling mode on the hydrophilic sphere ended with the vapour layer collapse marked by an explosive release of bubbles (Fig. 2c). This is followed by a short phase of rapid cooling in the nucleate boiling mode (Fig. 2d). Film-boiling on the hydrophobic sphere also ended with an almost instantaneous collapse of the vapour layer. However, for the superhydrophobic sphere no vapour layer collapse was observed. Instead, the vapour layer gradually relaxed over the entire sphere surface and a residual bubble dome remained on the sphere apex when the cooling was complete (Fig. 2b) and the sphere surface exhibited the silver sheen appearance indicative of a final Cassie state of the liquid adjacent to the sphere surface (Supplementary Fig. 3).

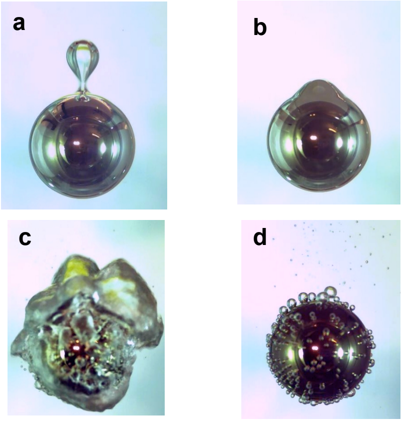

Figure 2 | High-speed camera snapshots of a 20 mm steel sphere cooling in water. a, Bubble pinch off from the vapour dome of hot sphere cooling in Leidenfrost regime. Example given is for superhydrophobic sphere cooling in 100 °C, at sphere temperature of about T_S = 200 °C. **b** The final state of the same superhydrophobic sphere cooled to pool temperature, T_S = 100 °C. **c, d,** Hydrophilic sphere cooling in 100 °C water at the moment of explosive transition from film boiling to nucleate boiling, T_S = 275°C (c) and during nucleate boiling T_S = 200°C (d). The sphere cooling events in 22 °C water are shown in Supplementary Movie 1 (hydrophilic sphere), Movie 2 (hydrophobic sphere) and Movie 3 (superhydrophobic sphere). The sphere cooling event in 100 °C water is shown in Supplementary Movie 4 (hydrophilic and superhydrophobic spheres).

The measured sphere temperature versus the immersion time is shown in Fig. 3. The superhydrophilic (Fig. 3a) sphere commenced cooling in the nucleate boiling regime and the temperature drops rapidly to the pool temperature. The cooling of the hydrophilic (Fig. 3a) and hydrophobic (Fig. 3b) sphere commenced in the Leidenfrost film-boiling regime. Then the vapour layer collapsed at the Leidenfrost point indicated by a sharp increase in the cooling rates at about 420 ºC for the hydrophilic sphere and at about 210 ºC for the hydrophobic sphere. However, for the superhydrophobic sphere, film-boiling is maintained down to the pool temperature (22 ºC) without vapour layer collapse and transition to nucleate boiling (Fig. 3b).

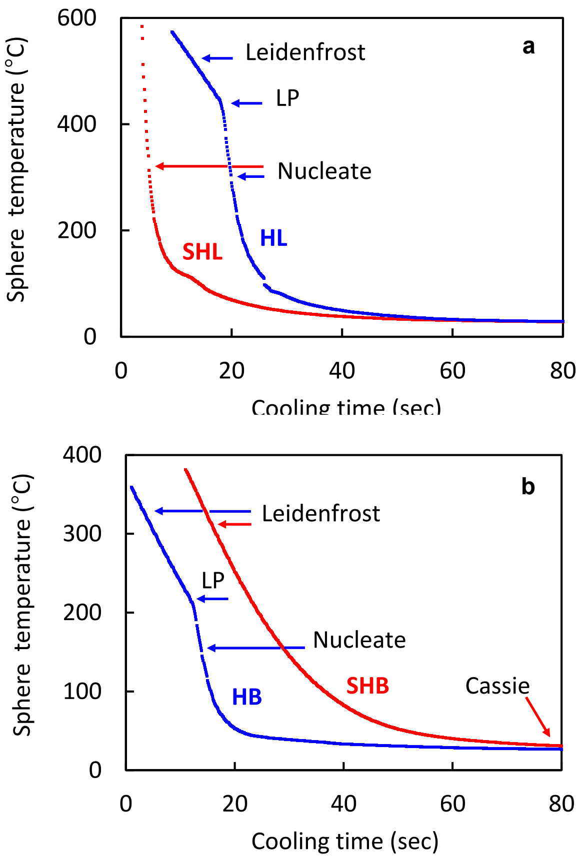

Figure 3 | Sphere temperature vs. cooling time for 20 mm steel sphere held in 22 °C water. a, Superhydrophilic sphere (contact angle < 10º, SHL red line) and hydrophilic surface sphere (contact angle ~30º, HL blue line) **b**, Hydrophobic surface sphere (contact angle ~100º, HB blue line) and superhydrophobic surface sphere (contact angle > 160º, SHB red line). The arrows on (a) and (b) indicates the Leidenfrost film boiling regime, Leidenfrost point (LP) transition, and nucleate boiling regime. The Leidenfrost transition temperature of the superhydrophilic case is higher than the displayed temperature scale in (a). In the superhydrophobic case the Leidenfrost state relaxed to Cassie state without passing through the nucleate boiling regime.

Cooling experiments at elevated water pool temperatures of 80 °C and 100 °C confirmed the same trends as the room-temperature cooling experiments with respect of the sphere hydrophobicity (Supplementary Fig. 5 and Supplementary Movie 4). In fact, as long as the water contact angle at room temperature exceeded 140º, achievable at textured superhydrophobic surfaces, no Leidenfrost transition was observed (Supplementary Fig. 7 and Fig. 8).

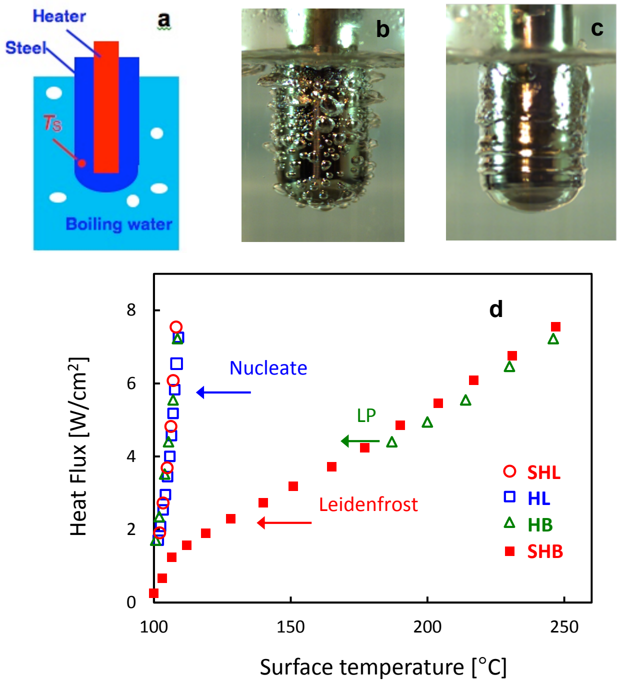

Figure 4 | Surface temperature vs. heat flux. a, Schematics of the immersion heater device**. b, c**, High-speed camera snapshots of the heater in boiling (100 ºC) water for the case of (b) hydrophobic surface in the nucleate boiling regime, at surface temperature T_S = 106°C and (c) superhydrophobic surface in the Leidenfrost regime, T_S = 210°C. **d**, Dependence of the heat flux on the heater surface temperature for superhydrophilic surface (SHL open circles, red), hydrophilic surface (HL open square, blue), hydrophobic surface (HB open triangles, green) and superhydrophobic surface (SHB solid squares, red) in the nucleate boiling and Leidenfrost vapour film boiling regimes.

Further characterizations of surface properties on the boiling transition were made using an immersion heater comprised of a cartridge heater placed inside a stainless steel cylinder (Fig 4a). The device was immersed in a beaker filled with water placed on a hot plate that heated the water to slow boiling, T_W = 100 °C. The surface temperature of the cylinder, T_S was measured with an inserted thermocouple under constant heat flux conditions by controlling the applied power to the heater. Temperature measurements were accompanied by high-speed video sequences.

Measured variations of the heat flux with surface temperature at steady state for the four types of surface wettability are shown in Fig. 4d. As expected for the low heat flux range used here, the heat exchange occurred in the nucleate boiling regime for the superhydrophilic and hydrophilic surfaces. However, as with the sphere-cooling experiments, the superhydrophobic surface was able to sustain a vapour layer in the Leidenfrost regime for all surface superheats. This is readily observed in both the appearance of the vapour layer and the magnitude of the increase in surface temperature with increasing heat flux (Fig. 4d).

When the temperature of the superhydrophobic cylinder was in equilibrium with the ambient water ($T_S = T_W = 100°C$), the surface appeared smooth and shiny. As the heater power increases, the appearance of surface ripples[6] accompanied a gradual transition to the Leidenfrost regime (Fig. 4c, Supplementary Fig. 10 and Supplementary Movie 5). Additional experiments with the immersion heater device detailed in the Supplementary Information indicated that for the superhydrophobic surface there was no hysteresis between heating-up and cooling-down experiments. Keeping the surface immersed in water for up to 24 hours did not alter the smooth transition to the Leidenfrost regime (Supplementary Fig. 11). Although, the surfaces appeared matte instead of shiny, suggesting that the vapour layer was not in a pure Cassie state, upon heating up, the surface returned smoothly to the Leidenfrost state (Supplementary Fig. 12). The same recovery property of superhydrophobi*c* surface has been recently demonstrated using electrophoresis[26].

For the hydrophobic surface, it was possible to maintain the Leidenfrost vapour regime only if before immersion the cylinder was overheated to about 350 °C and then maximizing the heater power upon immersion. But when the surface temperature was allowed to fall below about 170 °C, the Leidenfrost vapour layer collapsed and the boiling switched to the nucleate boiling branch (Fig. 4d).

Experiments with a stainless steel cup placed on a hot plate showed the same behavior as with the immersion heater device (Supplementary Fig. 14 and Fig. 15). The good agreement between experiments with heated spheres cooling in water, with the immersion heater and with water-in-a-cup confirm the independence on geometry and the universality of the superhydrophobic surface effect in stabilizing the Leidenfrost vapour layer (compare Fig. 4d with Supplementary Fig. 6b and Fig. 15).

By combining results for cooling experiments at constant initial heat content and high initial temperatures, and heating experiments at constant heating power but over a range of lower superheat temperatures, we have shown that the mode of heat transfer at the solid-liquid interface can be controlled by a combination of the surface morphology and surface chemistry of the solid surface. The observations for the hydrophilic and the hydrophobic surfaces are consistent with the standard transition between nucleate and film boiling[27]. The strong effect of the superhydrophilic surface in increasing the Leidenfrost temperature and enhancing boiling heat transfer has been also investigated recently [13]. However, we now show that for textured superhydrophobic surfaces the heat exchange always occurs in the presence of a Leidenfrost vapour layer within the film-boiling regime. This behavior represents a major departure from the characteristic form of the classical boiling heat transfer curve[10,28,29] of heat flux vs. surface superheat temperature. The currently accepted form of the boiling curve comprises of a critical heat flux maximum and a Leidenfrost point minimum that characterizes the transition between nucleate and film boiling. But at a textured superhydrophobic surface, the heat flux is a smoothly increasing function of superheat temperature due to the vapour layer that is always maintained at such surfaces (Supplementary Fig. 17).

The vapour layer on the superhydrophobic surface is sustained by the high surface roughness and porosity coupled with the intrinsic non-wetting, hydrophobicity due to surface chemical treatment. These are conditions for the existence of a large non-wetting vapour layer (see Supplementary Information discussion on stabilisation of vapour layers due to texture). Furthermore, the 3D nature of the surface roughness only permits small areas of direct contact between the peaks of the rough surface and the liquid interface. Contributions to the total heat transfer at such small areas are thus limited and any onset of heterogeneous nucleation of bubbles will simply be taken up in the surface vapour layer that in effect will contribute to a smooth transition to Leidenfrost regime. These conclusions are in complete accord with the observations we found in repeating Leidenfrost's experiments [1] of drop evaporation at heated surfaces. For hydrophobic surfaces we observed the classical transition from nucleate to film-boiling mode occur, whereas at superhydrophobic surfaces nucleate-boiling is absent at all superheats (Supplementary Fig. 16).

With the recent explosive development of both laboratory designed and commercially available textured surface coatings of superhydrophobic[23,24], superamphiphobic[8,9], anti-frost[7] or switchable hydrophobicity[30] properties the effect on the thermal exchange shown here opens possibilities for novel applications of these coatings ranging from the design of efficient heat exchange devices to aqueous drag reduction technologies.

METHODS SUMMARY

In cooling experiments we used stainless steel 20 mm diameter spheres (FRITSCH GmbH). In heating experiments we used an immersion heater or a 60 ml stainless steel cup. The immersion heater is a 24 mm diameter stainless steel hollow cylinder with an electric heater cartridge fitted inside. All stainless steel surfaces are modified as follows. Smooth hydrophilic surfaces are produced by cleaning with organic reagents. Smooth hydrophobic surfaces are produced by silanization with trichloro ([1H,1H,2H,2H perfluorooctyl] silane) . Textured superhydrophobic surfaces are produced by treatment with a commercial superhydrophobic coating agent (Glaco Mirror Coat "Zero", Soft 99 Co.). Textured superhydrophilic surfaces are produced by plasma cleaning of the surfaces previously treated with the superhydrophobic agent. A 2 mm hole is drilled into the spheres, the immersion heater cylinder wall or the bottom of the cup vessel to allow the insertion of a thermocouple probe to measure the surface temperature. In cooling experiments, the heated sphere is quenched in a water-filled vessel and the sphere temperature is recorded as function of time. In heating experiments, the cylindrical heater is immersed in water-filled glass beaker placed on a hot plate to control the water temperature and the heater surface temperature is measured as a function of the applied power to the heater cartridge in the cylinder. The heat transfer process on the sphere surface and the immersion heater surface is recorded using a high-speed video camera (Photron Fastcam SA-5). In the cup vessel experiments, the water-filled cup is placed on a hot plate and the vessel surface temperature is measured as a function of the hot plate temperature. The same setup is used to measure the evaporation time of water droplets placed on the bottom of the cup. Further details on the methods are available in the Supplementary Information.

REFERENCES:

1. Leidenfrost, J. G. *De Aquae Communis Nonnullis Qualitatibus Tractatus* (Duisburg, 1756). English translation: Wares, C. On the fixation of water in diverse fire. *Int. J. Heat Mass Transfer* **9**, 1153-1166 (1996).
2. Bernardin, J. D. & Mudawar, I. The Leidenfrost point: Experimental study and assessment of existing models. *Trans. ASME* **121**, 894-903 (1999).
3. Berthoud, G., Vapor explosions. *Annu. Rev. Fluid Mech.* **32**, 573-611 (2000).
4. Linke, H. *et al.* Self-propelled Leidenfrost droplets. *Phys. Rev. Lett.* **96**, 154502 (2006).
5. Lagubeau, N., Le Merrer, M., Clanet, C. & Quéré, D. Leidenfrost on a ratchet, *Nature Physics* **7**, 395-398 (2011)
6. Vakarelski, I. U., Marston, J. O., Chan, D. Y. C. & Thoroddsen S. T. Drag reduction by Leidenfrost vapor layers. *Phys. Rev. Lett.* **106**, 214501 (2011).
7. Mishchenko, L. *et al.* Design of ice-free nanostructured surfaces based on repulsion of impacting water droplets. *ACS Nano* **4**, 7699–7707 (2010).
8. Wong, T. S. *et al.* Bioinspired self-repairing slippery surfaces with pressure-stable omniphobicity. *Nature* **477**, 443- 447 (2011).
9. Deng, X. Mammen, L. Butt, H. J. & Vollmer, D. Candle soot as a template for a transparent robust superamphiphobic coating. *Science* **335**, 67- 70 (2012).
10. Patankar, N. A. Supernucleating surfaces for nucleate boiling and dropwise condensation heat transfer. *Soft Matter* **6**, 1613-1620 (2010).
11. Wang, C. H. & Dhir, V. K. Effect of surface wettability on active nucleation site density during pool boiling of water on a vertical surface. *ASME J. Heat Transfer* **115**, 659–669 (1993).
12. Takata, Y., Hidaka, A &Kohno M. Boiling from a super-water-repellent surface, *Proceedings of Fifth International Conference on Enhanced, Compact and Ultra-compact Heat Exchangers: Science, Engineering and Technology, Engineering Conferences International, Hoboken, NJ, USA, September 2005*, (Eds. Shah, R. K., Ishizuka, M., Rudy, T. M. & Wadekar, V. V.), 300-304 (2005).
13. Chen, R., *et al.* Nanowires for enhanced boiling heat transfer, *Nano Lett.* **9**, 548-553 (2009).
14. Liu, G. & Craig, V. S. J. Macroscopically flat and smooth superhydrophobic surfaces: Heating induced wetting transitions up to the Leidenfrost temperature. *Faraday Discuss.* **146**, 141-151 (2010).
15. Liu, G., Fu, L., Rode, A. V. & Craig, V. S. J. Water droplet motion control on superhydrophobic surfaces: Exploiting the Wenzel-to-Cassie transition. *Langmuir* **27**, 2595-2600 (2011).
16. Kim, H., Truong, B., Buongiomo, J. & Hu, L. On the effect of surface roughness height, wettability, and nanoporosity on Leidenfrost phenomena. *App. Phys. Letts.* **98**, 083121 (2011).
17. Zvirin, Y., Hewitt G. R. & Kenning, D. B. R. Boiling on free-falling spheres: Drag and heat transfer coefficients. *Exp. Heat Transfer* **3**, 185-214 (1990).
18. Rothstein, J. P. Slip on superhydrophobic surfaces. *Annu. Rev. Fluid Mech.* **42,** 89– 109 (2010).
19. Ceccio S. L. Friction drag reduction of external flows with bubble and gas injection. *Ann. Rev. Fluid Mech.* **42**, 183-203 (2010).
20. McHale, G., Newton M. I. & Shirtcliffe, N. J. Immersed superhydrophobic surfaces: Gas exchange, slip and drag reduction properties. *Soft Matter* **6**, 714–719 (2010).
21. Cassie, A. B. D. & Baxter, S. Wettability of porous surfaces. *Trans. Faraday Soc.* **40**, 0546–0550 (1944).
22. Patankar, N. A. On the modeling of hydrophobic contact angles on rough surfaces. *Langmuir* **19***,* 1249-1253 (2003).
23. Larmour, I. A., Bell, S. E. J. & Saunders, G. S. Remarkably simple fabrication of superhydrophobic surfaces using electroless galvanic deposition. *Angew. Chem. Int. Ed.* **46**, 1710 –1712 (2007).
24. Quéré, D. Wetting and roughness, *Annu. Rev. Mater. Res.* 38, 71–99 (2008)
25. Flynn, M. R. & Bush, J. W. M. Underwater breathing: the mechanics of plastron respiration *J. Fluid Mech.* **608**, 275–296 (2008).

26. Lee, C. & Kim, C.-J. Underwater restoration and retention of gases on superhydrophobic surfaces for drag reduction. *Phys. Rev. Lett.* **106**, 014502 (2011).
27. Dhir V. K. & Purohit G. P. Subcooled film-boiling heat transfer from spheres, *Nuclear Engineering and Design* **47,** 49-66 (1978).
28. Nukiyamam S. The maximum and the minimum values of heat Q transmitted from metal to boiling water under atmospheric pressure. *Journal Japan Sm. Mech. Engrs.* **37**, 367-314 (1934).
29. Witte L. C. & Lienhard, J. H. On the existence of two "transition" boiling cure. *Int. J. Heat Mass Transfer.* **35**, 771-779 (1982).
30. Celestini F. & Kirstetter G. Effect of an electric field on a Leidenfrost droplet. *Soft Matter* **8**, 5992–5995 (2012).

Supplementary Information is linked to the online version of the paper at www.nature.com/nature.

Acknowledgments We acknowledge G. D. Li from KAUST Electronic Workshop Core Lab facility for assistance in setting up the sphere cooling experiments, L. Chen and B. Chew from KAUST Advanced Nanofabrication, Imaging and Characterization Core Lab facilities for assistance in AFM and SEM imaging characterization of the superhydrophobic coating.

Author Contributions I.U.V. conceived research and designed the experiments. I.U.V. and J.O.M. carried out the experiments. N.A.P., D.Y.C.C. and S.T.T. contributed with discussions, analysis and theoretical interpretation of the experimental results. I.U.V., D.Y.C.C. and N.A.P. wrote the manuscript. All authors edited the manuscript.

Author Information Reprints and permissions information is available at www.nature.com/reprints. Readers are welcome to comment on the online version of this article at www.nature.com/nature. The authors declare no competing financial interests.

Correspondence and requests for materials should be addressed to I.U.V. (ivanuriev.vakarelski@kaust.edu.sa) or N.A.P. (n-patankar@northwestern.edu).